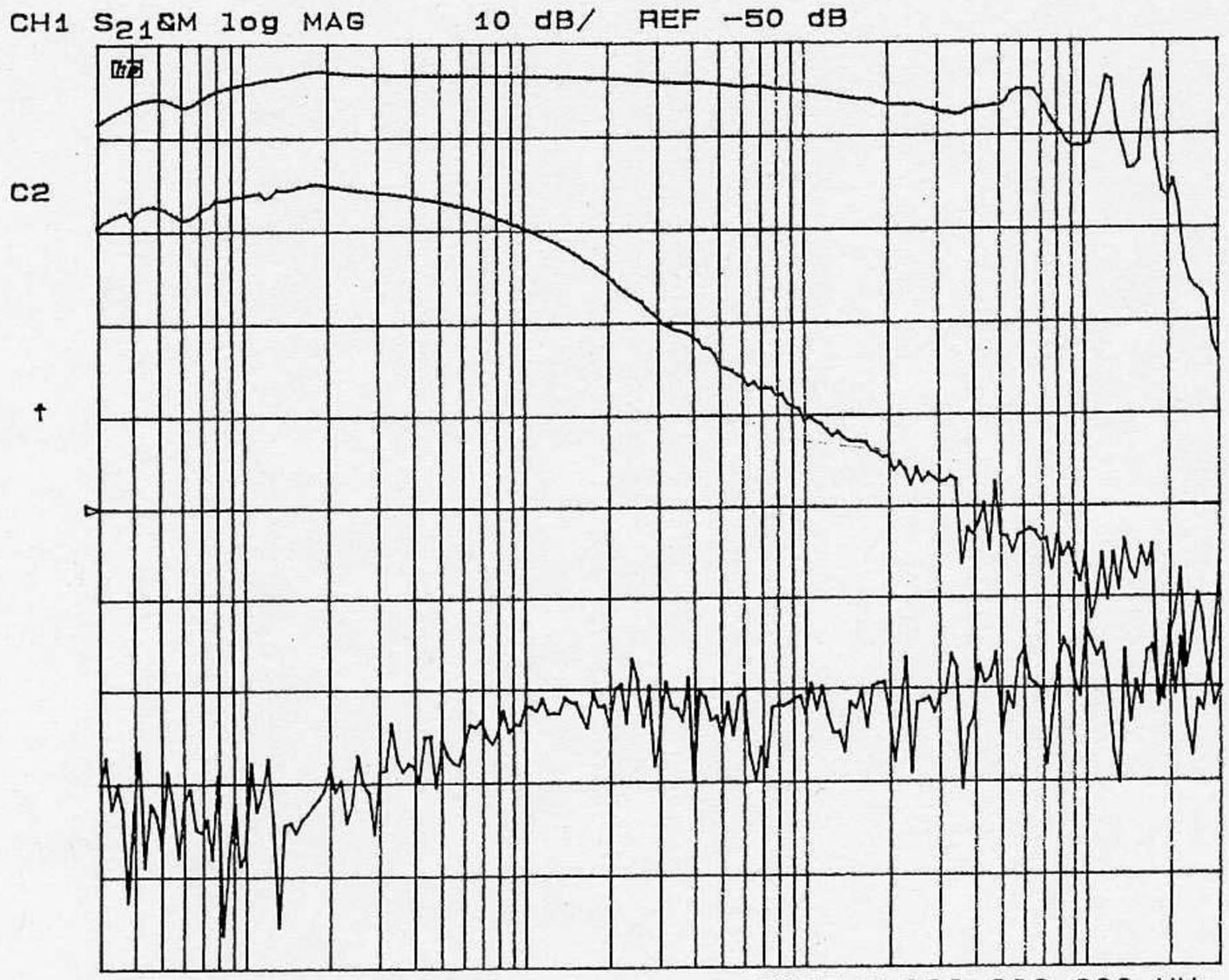

Figure 5 Measurement results of *p-i-n*–PD-TG optoelectronic switch. Top trace, *p-i-n*–PD and TG in the on states; middle trace, *p-i-n*–PD in the off state and TG in the on state; bottom trace, *p-i-n*–PD and TG in the off states

low frequencies. Isolation levels of 70 and 55 dB are obtained at 300 KHz and 1.0 GHz, respectively. It is demonstrated that the frequency dependence of the *p-i-n*–PD isolation is complemented by that of the TG.

4. CONCLUSION

In conclusion, a novel optoelectronic switch has been demonstrated theoretically and experimentally by introducing a GaAs MESFET TG between the switching *p-i-n*–PD and load. Combining the high isolation characteristics of the TG at low frequencies and that of *p-i-n*–PD switch at high frequencies, we demonstrated an optoelectronic switch operating from dc to the microwave frequency range. Measured isolation levels more than 70 dB at 300 KHz and 55 dB at 1.0 GHz were obtained. The *p-i-n*–PD-TG optoelectronic switch has potential applications for both optical and microwave signal processing with very high isolation and wide bandwidth.

REFERENCES

1. R. I. MacDonald and E. H. Hara, "Optoelectronic Broadband Switching Array," *Electron. Lett.*, Vol. 14, 1978, pp. 502–503.
2. E. H. Hara and R. I. MacDonald, "A Broadband Optoelectronic Microwave Switch," *IEEE Trans. Microwave Theory Tech.*, Vol. MTT-28, No. 6, 1980, pp. 662–665.
3. M. Veilleux and R. I. MacDonald, "An Optoelectronic Switch Matrix with High Isolation," *J. Lightwave Technol.*, Vol. 10, No. 7, 1992, pp. 988–991.
4. S. R. Forrest, G. L. Tangonan, and V. L. Jones, "A Simple 8 × 8 Optoelectronic Crossbar Switch," *J. Lightwave Technol.*, Vol. 7, No. 4, 1989, pp. 607–614.
5. R. I. MacDonald, "Optoelectronic Matrix Switching," *Can. J. Phys.*, Vol. 67, 1989, pp. 389–393.
6. R. I. MacDonald, "Switched Optical Delay Line Signal Processor," *J. Lightwave Technol.*, Vol. 5, No. 6, 1987, pp. 856–861.
7. R. I. MacDonald and S. S. Lee, "Photodetector Sensitivity Control for Weight Setting in Optoelectronic Neural Networks," *Appl. Opt.*, Vol. 30, No. 2, 1991, pp. 176–178.
8. B. E. Swekla and R. I. MacDonald, "Optoelectronic Transversal Filter," *Electron. Lett.*, Vol. 27, No. 19, 1991, pp. 1769–1770.
9. R. S. Pengelly, *Microwave Field Effect Transistor—Theory, Design and Application*, John Wiley & Sons, Inc., New York, 1982.
10. R. I. MacDonald and E. H. Hara, "Switching with Photodiodes," *IEEE J. Quantum Electron.*, Vol. QE-16, No. 3, 1980, pp. 289–295.
11. Y. Liu, S. R. Forrest, G. L. Tangonan, R. A. Jullens, R. Y. Loo, V. L. Jones, D. Persechini, J. L. Pikulski, and M. M. Johnson, "Very High Bandwidth $In_{0.53}Ga_{0.47}As$ *pin* detector arrays," *IEEE Photon. Technol. Lett.*, Vol. PTL-3, No. 10, 1991, pp. 931–933.

Received 5-9-95

Microwave and Optical Technology Letters, 10/2, 88–91

CCC 0895-2477/95

MODIFIED ANALYSIS OF CONICAL HORNS

Jens Bornemann
Laboratory for Lightwave Electronics,
Microwaves and Communications (LLiMiC)
Department of Electrical and Computer Engineering
University of Victoria
Victoria, British Columbia, Canada V8W 3P6

KEY TERMS

Conical horn antennas, antenna gain, antenna feeds

ABSTRACT

A modified analysis of conical horns is presented that takes into account the true phase relationships between the feeding waveguide, the conical horn section, and the aperture phase variation. It is demonstrated that, especially for low-gain applications, an accurate account of the aperture phase error results in higher gains than those obtained by widely used design methods—or that a slightly shorter horn is obtained for identical gain specifications. Comparisons with measured data reveal the advantage of this relatively simple analysis compared with techniques involving the conical waveguide mode spectrum. © *1995 John Wiley & Sons, Inc.*

I. INTRODUCTION

Due to excellent earlier work, both technical and experimental, and the focus on currugated horn antennas in recent years, the conical waveguide horn has received only moderate attention over the past decades. An experimental investigation on the radiation characteristics of conical horns was published as early as 1939 [1]. A theory based on the mode spectrum of the conical waveguide [2] obtained good agreement with those measurements up to total flare angles of approximately 40 degrees. At higher flare angles, the theory fails due to the neglect of the cos θ variation of the aperture field. In 1950, King [3] presented design graphs for optimum conical horns that follow the well-known gain maxima obtained for fixed horn lengths and varying aperture dimensions. These graphs have been reprinted in many texts and handbooks on antenna theory, for example, [4–6], and have since become the standard design tools for conical horns.

However, the theory used to create the design graphs is based on plane-wave propagation within the horn and purely geometrical relationships for the aperture phase error. As was pointed out earlier for E-plane sectoral horns [7] and, more recently, for pyramidal horns [8], the neglect of dispersion within both the feeding waveguide and the horn section leads to an overestimation of the aperture phase error. Because the same principles apply but obviously have not been investigated with respect to the conical horn, this article presents the analysis associated with this approach. It is demonstrated that, especially for low-gain conical horns, the conventional prediction of the gain is poor, so that designs according to [3] might not be optimally compact. A modified design graph is presented to provide the design engineer with some guidelines regarding the validity range of the conventional approach.

II. THEORY

The calculation of the aperture phase error for the conical horn is similar to that for the pyramidal horn in [8], and therefore only the basic steps will be presented here. For details the reader is referred to [8].

The geometry of the conical horn is depicted in Figure 1. The phase shift between the phase center and the aperture is given by

$$\phi_r = \frac{2\pi}{\lambda_{g11}}(L-h) + 2\pi\int_0^h \sqrt{\frac{1}{\lambda^2} - \frac{1}{[2A(z)]^2}}\, dz. \quad (1)$$

The first term in (1) represents the contribution of the fundamental TE_{11} mode in the feeding circular waveguide, where

$$\lambda_{g11} = \frac{\lambda}{\sqrt{k^2 - k_c^2}} = \frac{\lambda}{\sqrt{k^2 - \left(\frac{p'_{11}}{a}\right)^2}}, \quad (2)$$

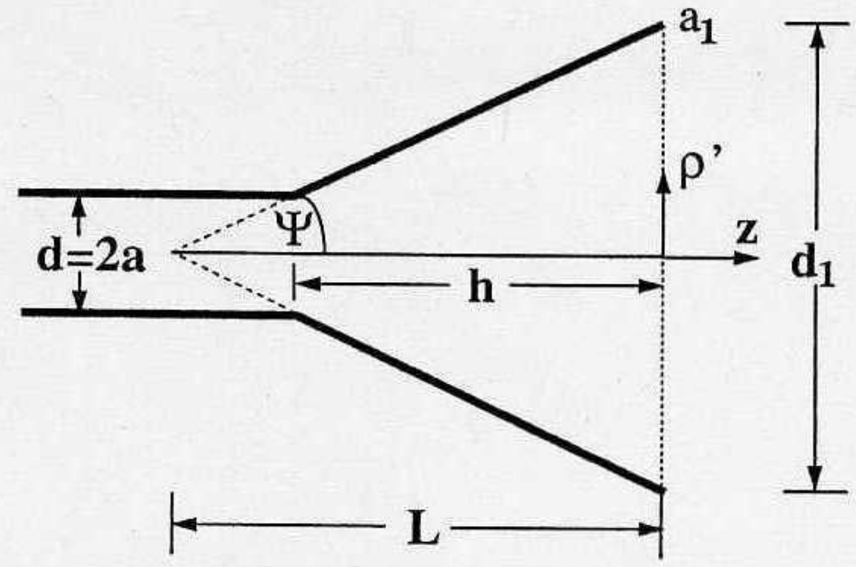

Figure 1 Geometry of conical waveguide horn

and p'_{11} is the first zero of the derivative of Bessel function $J_1(x)$. The second term in (1) is the phase shift along the conical horn of length h. An integral of this type is solved analytically in [8]. In this case, the solution can be obtained by subsituting

$$A(z) = \frac{\pi}{p'_{11}}(a + z\tan\Psi). \quad (3)$$

The variation of the phase error over the aperture is finally given by

$$\phi_{ap}(\rho') = \phi_r\left[\frac{1}{\cos\{\arctan(\rho'/L)\}} - 1\right], \quad (4)$$

and is assumed to distort the desired TE_{11} mode field distribution in the aperture. The electric field is oriented such that it is maximum at $\phi = \phi' = \pi/2$ (the prime indicating the aperture). Thus the far-field components can be evaluated from

$$E_\theta \propto \sin\phi\left(1 + \frac{\beta_{11}}{k}\cos\theta\right)(I_{\theta 1} + I_{\theta 2}), \quad (5)$$

$$E_\phi \propto \cos\phi\left(\frac{\beta_{11}}{k} + \cos\theta\right)(I_{\phi 1} + I_{\phi 2}), \quad (6)$$

where the factor

$$\frac{\beta_{11}}{k} = \sqrt{1 - \left(\frac{k_{c1}}{k}\right)^2} = \sqrt{1 - \left(\frac{p'_{11}/a_1}{k}\right)^2} \quad (7)$$

is approximately, though not exactly, unity and reflects the fact that the wave impedance of free space differs from that of the TE_{11} mode in the circular aperture. Note that the effect of (7) in (5) and (6) increases for decreasing aperture dimensions, that is, for lower gain. After some manipulation, integrals $I_{\theta,\phi,1,2}$ in (5) and (6) can be reduced to

$$I_{\theta 1} = \int_0^{a_1} \frac{J_1(k_{c1}\rho')}{k_{c1}}\left[J_0(k\rho'\sin\theta) - \frac{J_1(k\rho'\sin\theta)}{k\rho'\sin\theta}\right] \times e^{-j\phi_{ap}(\rho')}\, d\rho', \quad (8)$$

$$I_{\theta 2} = \int_0^{a_1} \left[\rho' J_0(k_{c1}\rho') - \frac{J_1(k_{c1}\rho')}{k_{c1}} \right] \times \frac{J_1(k\rho' \sin\theta)}{k\rho' \sin\theta} e^{-j\phi_{ap}(\rho')}\, d\rho', \quad (9)$$

$$I_{\phi 1} = \int_0^{a_1} \frac{J_1(k_{c1}\rho')}{k_{c1}} \frac{J_1(k\rho' \sin\theta)}{k\rho' \sin\theta} e^{-j\phi_{ap}(\rho')}\, d\rho', \quad (10)$$

$$I_{\phi 2} = \int_0^{a_1} \left[\rho' J_0(k_{c1}\rho') - \frac{J_1(k_{c1}\rho')}{k_{c1}} \right] \times \left[J_0(k\rho' \sin\theta) - \frac{J_1(k\rho' \sin\theta)}{k\rho' \sin\theta} \right] e^{-j\phi_{ap}(\rho')}\, d\rho', \quad (11)$$

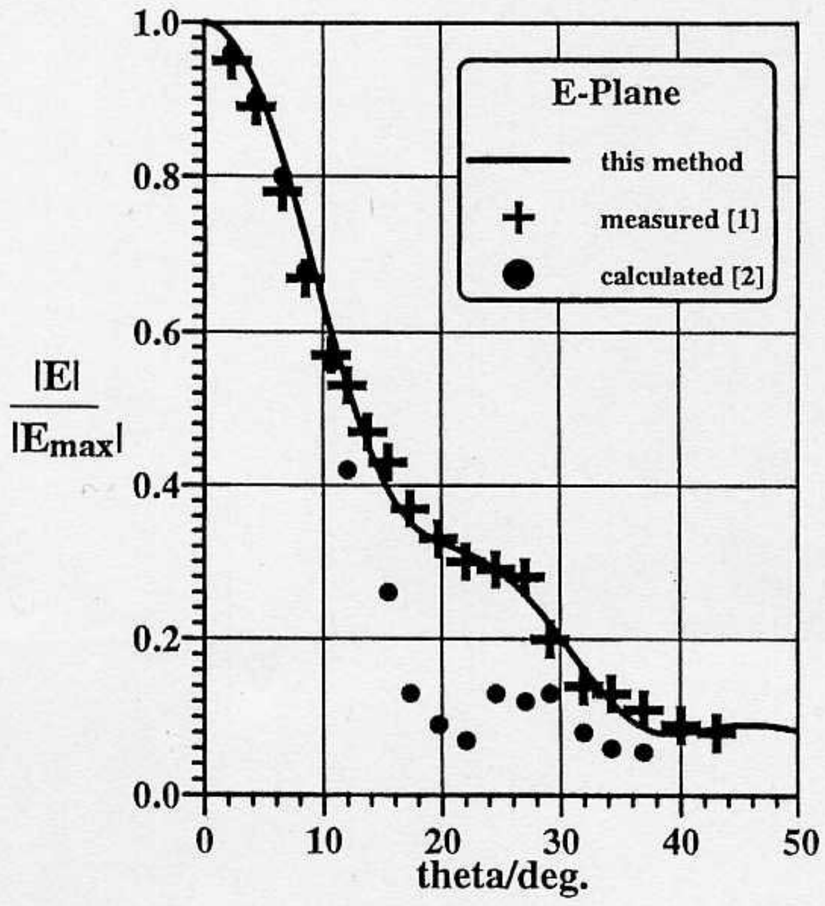

(a)

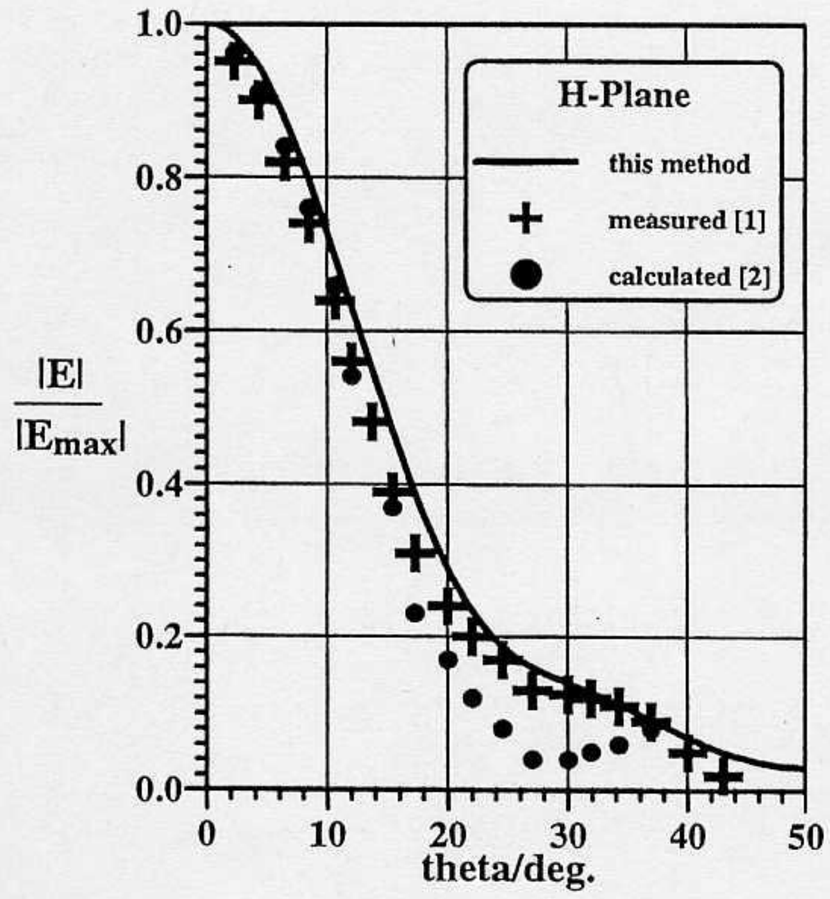

(b)

Figure 2 Comparison of radiation characteristics with measured [1] and calculated [2] values. (Measured data are taken from [2] as Cartesian reproductions of polar presentations in [1].) Dimensions: $d = 12.4$ cm, $d_1 = 54.8$ cm, $h = 50.0$ cm. (a) E plane, (b) H plane

and are evaluated numerically by a Gauss-Legendre routine, for example, [9]. A rule of thumb on the number of integration points required is given by 2.5 times the gain in decibels obtained from the conventional aperture formula [4, 5].

III. RESULTS

Figure 2 compares radiation characteristics of this analysis with measurements in [1] and calculations in [2]. Within the readability of the data presented in [2] (which also includes reproductions in Cartesian coordinates of the measured polar plots in [1]), the agreement between this method and measurements is very good. Note that due to the total flare angle of approximately 46° deg and—as mentioned earlier—the neglect of a $\cos\theta$ variation in [2], the calculated characteristics obtained with the conical waveguide approach of [2] show unacceptably high discrepancies with measurements.

The influence of the diameter of the feeding circular waveguide, which is associated with the aperture phase error by the first term of (1), is demonstrated in Figure 3. Because the reference values [3] are obtained under the assumption of a plane-wave propagation in the horn, the assumed free-space wavelength λ at any location along the horn is always shorter than the actual guide wavelength λ_g at that location. Consequently, the phase error obtained with the present technique, which takes the influences of the feeding waveguide and that of the widening horn section adequately into account, produces less aperture phase error and, therefore, higher gain. The difference between λ and λ_g increases toward lower frequencies (or smaller d/λ), hence leading to slightly higher gains (dashed lines in Figure 3). Note that the monomode range of the fundamental TE_{11} mode in a circular waveguide lies between 0.59 and 0.76 in terms of d/λ. As pointed out for pyramidal horns in [8], a significant influence of this effect is only observed for short, that is, low-gain horns ($L/\lambda = 1$ in Figure 3). For longer horns and flare angles associated with near-optimum designs, this effect is less and less pronounced as the actual electromagnetic field within the horn more and more resembles that of a spherical wave. Consequently, the

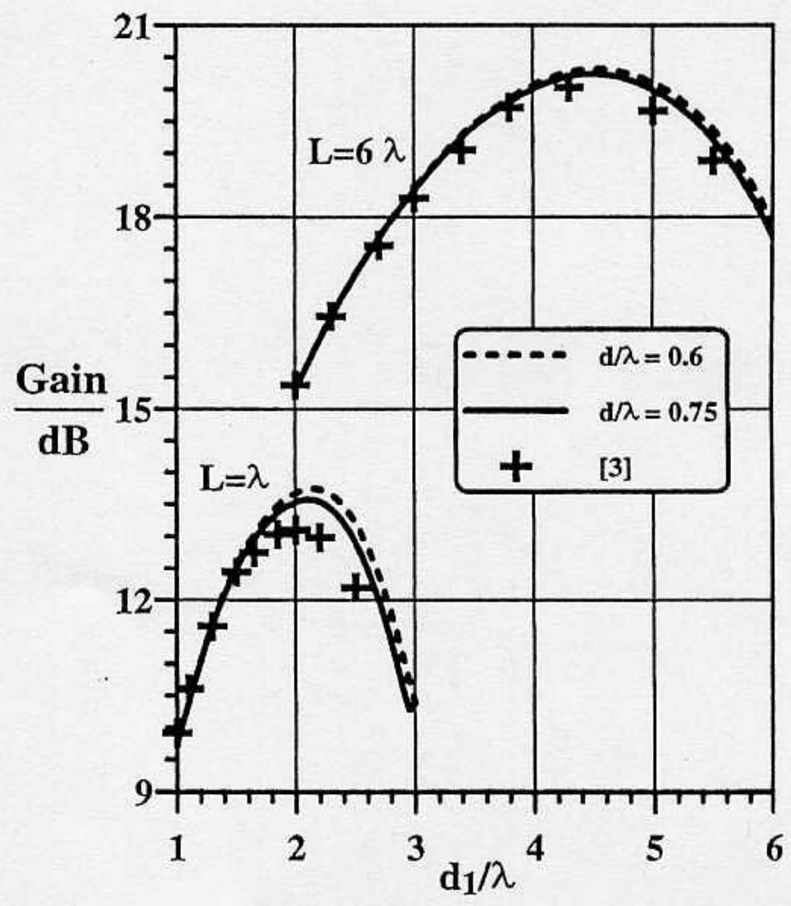

Figure 3 Influence of the feeding circular waveguide and comparison of gain calculations with [3]

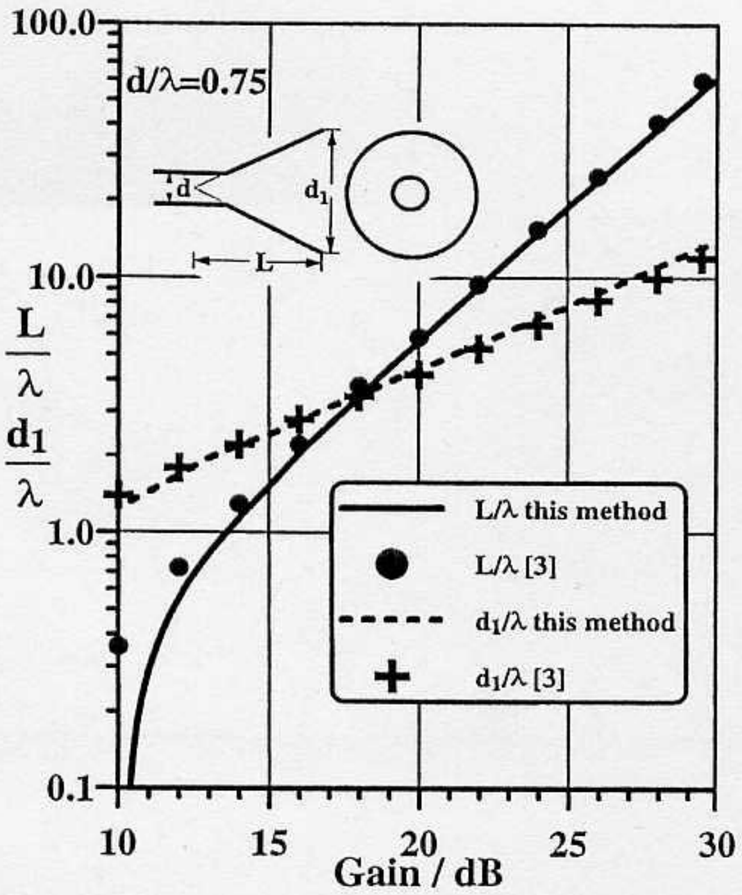

Figure 4 Length and aperture dimensions of optimum conical horns for specified gain

differences between dashed and solid lines and the reference values [3] decrease (e.g., $L/\lambda = 6$ in Figure 3).

Figure 4 displays optimum conical horn dimensions for a specified gain. The procedure to obtain these data is identical to that described in [3], where for a given length L/λ, the aperture diameter d_1/λ is optimized for maximum gain. Good agreement is again obtained between this theory and data of [3]. At low gains, however, the classical approach [3] fails to reliably predict the horn length, or, in other words, leads to longer than optimum designs.

IV. CONCLUSIONS

It is demonstrated that the accurate calculation of the aperture phase error of conical horns leads to shorter designs than previously considered optimum. However, the effect is only visible in low-gain applications (i.e., below 15 dB), where the commonly applied plane-wave theory is no longer a reasonable assumption and, therefore, fails to accurately predict the antenna gain. Longer horns with near-optimum flare angle are only marginally affected. The modified analysis produces results that are in excellent agreement with measurements.

REFERENCES

1. G. C. Southworth and A. P. King, "Metal Horns as Directive Receivers of Ultra-Short Waves," *Proc. IRE*, Vol. 27, Feb. 1939, pp. 95–102.
2. M. G. Schorr and F. J. Beck, Jr., "Electromagnetic Field of the Conical Horn," *J. Appl. Phys.*, Vol. 21, Aug. 1950, pp. 795–801.
3. A. P. King, "The Radiation Characteristics of Conical Horn Antennas," *Proc. IRE*, Vol. 38, March 1950, pp. 249–251.
4. W. L. Stutzman and G. A. Thiele, *Antenna Theory and Design*, John Wiley & Sons, New York, 1981.
5. C. A. Balanis, *Antenna Theory: Analysis and Design*, John Wiley & Sons, New York, 1982.
6. E. A. Wolff, *Antenna Analysis*, Artech House, Norwood, May 1988.
7. E. V. Jull and L. E. Allan, "Gain of the E-Plane Sectoral Horn—A Failure of the Kirchhoff Theory and a New Proposal," *IEEE Trans. Antennas Propagat.*, Vol. AP-22, March 1974, pp. 221–226.
8. D. C. Hawkins and F. Thompson, "Modifications to the Theory of Waveguide Horns," *IEE Proc. Pt.-H*, Vol. 140, Oct. 1993, pp. 381–386.
9. W. H. Press, B. P. Flannery, S. A. Teukolsky, and W. T. Vetterling, *Numerical Recipes—The Art of Scientific Computing*, Cambridge University Press, Cambridge, 1989.

Received 5-4-95

Microwave and Optical Technology Letters, 10/2, 91–94

CCC 0895-2477/95

FAST ITERATIVE ALGORITHM FOR THE FINE DETAIL ANALYSIS OF PLANAR SCATTERERS

Bezalel Finkelstein and Raphael Kastner
Department of Physical Electronics
Faculty of Engineering
Tel Aviv University
Tel Aviv 69978, Israel

KEY TERMS

Method of moments, iterative techniques, conjugate gradient, high resolution

ABSTRACT

A very efficient iterative algorithm is presented for the analysis of planar scatterers at the very fine detail regime. The mechanisms causing slow convergence in other techniques have been identified and corrected. The resultant algorithm converges very fast for problems with fine details sampled faster than 0.001λ, where other methods fail. © 1995 John Wiley & Sons, Inc.

1. INTRODUCTION

Iterative algorithms have been enjoying a renewed interest recently due to the appearance of new methods such as the fast multipole method (FMM) [1–4], multilevel computations [5, 6] and reduced representation of matrices [7] for rapid computation of matrix-vector multiplication. This operation is considered the bottleneck of each iteration step; however, the rate of convergence is also of primary importance. In this work we are considering a method for speeding up the convergence of iterative solutions for the class of planar and (potentially stacked planar) structures. This problem has been addressed in the past by such algorithms as the spectral iterative technique (SIT) [8–12] and the conjugate gradient method as formulated in the spectral domain (CG-FFT) [13–23]. These methods are sensitive to the intricacy of the structure and to the sampling interval. The finer the detail of the structure, and the higher the resolution, the slower convergence will be. The SIT tends to diverge in some extreme cases (see an example in [10]), whereas the CG-FFT process stagnates, and eventually, with the addition of round-off errors and loss of orthogonality, can also diverge [19]. Convergence can be enhanced for CG- and SIT-related techniques by such means as the following: (a) the use of a relaxation factor [10, 11]; (b) van den Berg's CST and CCST [13], which, like the SIM [19], make use of the inverse operator as in the SIT in conjunction with minimization loops; (c) the Mackay and McCowen method [20], which